

# Nuclear effects in photoproduction of heavy quarks and vector mesons in ultraperipheral PbPb and $p$ Pb collisions at energies available at the CERN Large Hadron Collider

Adeola Adeluyi and C. A. Bertulani

*Department of Physics & Astronomy, Texas A&M University-Commerce, Commerce, Texas 75428, USA*

M. J. Murray

*Department of Physics & Astronomy, University of Kansas, Lawrence, Kansas 66045-7582, USA*  
(Received 30 August 2012; revised manuscript received 7 October 2012; published 22 October 2012)

The comparison of photoproduction cross sections for  $c\bar{c}$  and  $b\bar{b}$  in PbPb and  $p$ Pb collisions can show sensitivity to nuclear shadowing effects. The photoproduction of vector mesons is even more sensitive to the underlying gluon distributions. In this study we present the cross sections and rapidity dependence of the photoproduction of heavy quarks and the exclusive production of vector mesons in ultraperipheral  $p$ Pb and PbPb collisions at the CERN Large Hadron Collider at  $\sqrt{s_{NN}} = 5$  TeV and  $\sqrt{s_{NN}} = 2.76$  TeV, respectively. The potentials of using these processes for constraining nuclear gluon shadowing are explored. It is found that the photoproduction of  $J/\psi$  and  $\Upsilon$  in PbPb collisions in particular exhibits very good sensitivity to gluon shadowing.

DOI: [10.1103/PhysRevC.86.047901](https://doi.org/10.1103/PhysRevC.86.047901)

PACS number(s): 24.85.+p, 25.30.Dh, 25.75.-q

In view of recent and upcoming experiments at the Large Hadron Collider (LHC) at CERN, we consider the inclusive photoproduction of heavy quarks ( $c\bar{c}$  and  $b\bar{b}$ ) and the exclusive elastic production of vector mesons [ $J/\psi$  and  $\Upsilon(1s)$ ] in ultraperipheral PbPb and  $p$ Pb collisions at  $\sqrt{s_{NN}} = 2.76$  and 5 TeV, respectively. The theoretical framework used for our calculations has been described in two recent publications [1,2]. The method consists of using the strong electromagnetic fields generated in relativistic heavy-ion collisions [3,4] to produce particles in  $\gamma$ -nucleus interactions. The large energies of the virtual photons produced in such reactions has stimulated many studies of the photoproduction of heavy mesons. Previously, we have investigated the sensitivity of the photoproduction of heavy quarks and the exclusive production of vector mesons at higher LHC energies to varying severity of gluon modifications [1,2]. This idea, originally proposed in Ref. [5], can be used to constrain parton distribution functions from data on the photoproduction of heavy quarks and of vector mesons.

All four of the large LHC experiments, ALICE, ATLAS, CMS, and LHCb, have the capability to measure  $J/\psi$  and  $\Upsilon$ , [6–12]. So far most LHC measurements have been in the muon channel. The calculations presented in the present paper are reported in terms of rapidity distributions  $d\sigma/dy$  in the center-of-mass frame. For PbPb collisions at the LHC this is the same as the laboratory frame but for  $p$ Pb collisions the proton and the lead beams have the same magnetic rigidity, which implies that the center of mass is shifted with respect to the laboratory frame by  $\delta y = 0.5 \ln(208/82) = 0.47$ . This rapidity shift presents both a challenge and an opportunity for the experiments. The acceptance of both CMS and ATLAS is symmetric around  $y_{lab} = 0$  and extends up to  $y_{lab} \approx 2.5$ . The strong magnetic fields and the large amount of material before the muon stations imply that only muons with a minimum momenta of order 5 GeV/ $c$  fire the trigger and this causes both ATLAS and CMS to only reconstruct  $J/\psi$  with a minimum transverse momentum,  $p_T$ , near  $y_{lab} = 0$ . However, at  $y_{lab} \approx 2.5$  both experiments can reconstruct  $J/\psi$ s

down to  $p_T = 0$ . The extra mass of the  $\Upsilon$  means that both CMS and ATLAS have acceptance down to  $p_T = 0$  over their whole rapidity range. Both ALICE and LHCb have asymmetric muon detectors with acceptances down to  $p_T = 0$  for  $2.5 \leq y_{lab} \leq 4.0$  (ALICE)  $2 \leq y_{lab} \leq 4.5$  (LHCb). If it were possible for these collaborations to take both  $p + Pb$  and  $Pb + p$  data then almost the complete phase space for ultraperipheral quarkonia production could be mapped out.

In the present work we follow closely the approach presented in Ref. [2]. All input parameters (except those related to energy), computational details, and references therein are applicable to the current study. We use the same sets of nuclear and photon parton distributions: MSTW08 [13], EPS08 [14], EPS09 [15], and HKN07 [16] for nucleon/nucleon parton distributions and GRV [17], SaS1D [18], and CJK2 [19] for photon parton distributions. The characteristics of these distributions, especially the disparities in the strength of the nuclear modifications of their gluon content, have been treated in detail in Ref. [2]. Because in general the features and trends of the results obtained in the previous study are faithfully reproduced in the present work, the discussions and comments presented therein are also valid and the reader is therefore referred to Ref. [2] for detailed exposition. We focus mainly on presenting the results, and hence in this respect the present report serves to augment and supplement the previous study contained in Ref. [2].

Let us first consider the photoproduction of heavy quarks in ultraperipheral  $p$ Pb and PbPb collisions where two rather different production mechanisms (direct and resolved) are present. In the direct mechanism the incident photon interacts directly with the target (nucleus or proton) whereas in the resolved mechanism the incident photon first fluctuates into a quark-antiquark pair (or even more complicated partonic configuration) which then subsequently interacts hadronically with the target. At leading order the direct production involves only the gluon distributions in the target while the resolved production requires the distributions of light quarks and gluons in both photons and targets. The total production cross

TABLE I. Cross sections (in  $\mu\text{b}$ ) for photoproduction of  $c\bar{c}$  and  $b\bar{b}$  in ultraperipheral  $p\text{Pb}$  collisions at  $\sqrt{s_{NN}} = 5.0$  TeV.

|            | PDF               | Direct | Resolved |      |      |      |
|------------|-------------------|--------|----------|------|------|------|
|            |                   |        | SaS1d    | GRV  | CJK  |      |
| $c\bar{c}$ | $\gamma p$        | MSTW08 | 3250     | 323  | 534  | 665  |
|            |                   | MSTW08 | 362      | 58   | 98   | 118  |
|            | $\gamma\text{Pb}$ | EPS08  | 238      | 50   | 85   | 101  |
|            |                   | EPS09  | 288      | 53   | 91   | 108  |
| $b\bar{b}$ | $\gamma p$        | MSTW08 | 18.0     | 3.32 | 4.56 | 5.61 |
|            |                   | MSTW08 | 2.80     | 0.90 | 1.29 | 1.58 |
|            | $\gamma\text{Pb}$ | EPS08  | 2.30     | 0.87 | 1.26 | 1.54 |
|            |                   | EPS09  | 2.50     | 0.88 | 1.28 | 1.56 |

sections and rapidity distributions are of course the sum of the contributions from both processes. As in Ref. [2] we present the cross sections for three nuclear parton distributions (MSTW08, EPS08, and EPS09) and the three photon parton distributions listed above. Also, for convenience, only the rapidity distributions using the GRV photon distributions are presented.

In Table I we present the direct and resolved cross sections for both  $\gamma p$  and  $\gamma\text{Pb}$  components of  $c\bar{c}$  and  $b\bar{b}$  production in  $p\text{Pb}$  collisions. The respective  $\gamma p$  and  $\gamma\text{Pb}$  rapidity distributions and their sums are displayed in Fig. 1. For both  $c\bar{c}$  and  $b\bar{b}$  production the  $\gamma p$  component is dominant due to the larger photon flux from the nucleus, leading to asymmetric rapidity distributions skewed towards the right, in line with the convention adopted in Ref. [2]. While the influence of nuclear shadowing is somewhat discernible in the  $\gamma\text{Pb}$  component of  $c\bar{c}$  photoproduction, this effect is minimized when one considers total rapidity distributions due to the smallness of the  $\gamma\text{Pb}$  component relative to the dominant

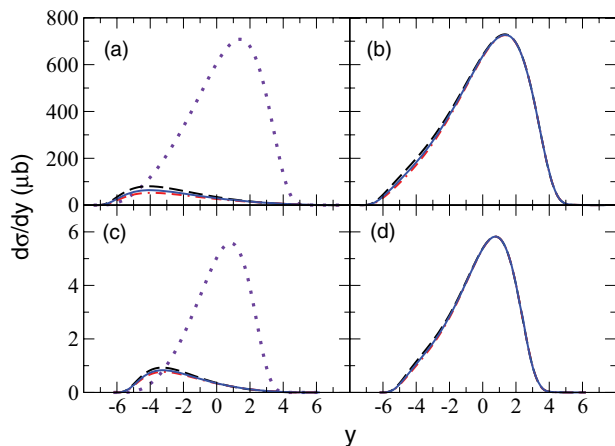


FIG. 1. (Color online) Rapidity distributions of  $c\bar{c}$  (top) and  $b\bar{b}$  (bottom) photoproduction in  $p\text{Pb}$  collisions at  $\sqrt{s_{NN}} = 5.0$  TeV using the GRV photon parton distributions. Panels (a) and (c) show the  $\gamma p$  and  $\gamma\text{Pb}$  contributions separately while panels (b) and (d) show the sum. The dotted lines depict the  $\gamma p$  contributions while the dashed (MSTW08), solid (EPS09), and dash-dotted (EPS08) lines correspond to  $\gamma\text{Pb}$  contributions with no shadowing, moderate shadowing, and strong shadowing, respectively.

TABLE II. Cross sections for photoproduction of  $c\bar{c}$  (in mb) and  $b\bar{b}$  (in  $\mu\text{b}$ ) in ultraperipheral PbPb collisions at the LHC.

|                              | PDF    | Direct | Resolved |       |       |
|------------------------------|--------|--------|----------|-------|-------|
|                              |        |        | SaS1d    | GRV   | CJK   |
| $c\bar{c}$ (mb)              | MSTW08 | 570.1  | 39.5     | 64.1  | 81.3  |
|                              | EPS08  | 469.8  | 39.4     | 64.1  | 81.0  |
|                              | EPS09  | 511.1  | 39.6     | 64.5  | 81.6  |
| $b\bar{b}$ ( $\mu\text{b}$ ) | MSTW08 | 2277.0 | 293.6    | 388.5 | 467.8 |
|                              | EPS08  | 2280.0 | 310.5    | 413.5 | 501.1 |
|                              | EPS09  | 2291.8 | 304.2    | 404.3 | 489.1 |

$\gamma p$  component. In view of this,  $c\bar{c}$  photoproduction in  $p\text{Pb}$  collisions could potentially serve as a good normalizer for the equivalent  $c\bar{c}$  photoproduction in PbPb collisions when effects due to differences in photon flux are taken into account. As evident from both Table I and Fig. 1, nuclear effects are rather unimportant in  $b\bar{b}$  photoproduction, because all three  $\gamma\text{Pb}$  rapidity distributions practically overlap. On the other hand the resolved component is relatively more significant than that in  $c\bar{c}$  production. This attribute, in conjunction with negligible sensitivity to nuclear effects and enhanced sensitivity to photon parton distributions as evinced in Table I suggests the potential for  $b\bar{b}$  photoproduction to be of some use in constraining photon parton distributions.

The corresponding cross sections and rapidity distributions for PbPb collisions are shown in Table II and Fig. 2. Here the participants are identical and each Pb nucleus can act as both the source and the target of photons. Consequently the photon flux is the same and the rapidity distributions are symmetric around midrapidity ( $y = 0$ ). For  $c\bar{c}$  production the effect of shadowing is quite appreciable especially in the rapidity interval  $-2 < y < 2$ , and thus this interval offers good constraining potential. The effect of antishadowing is

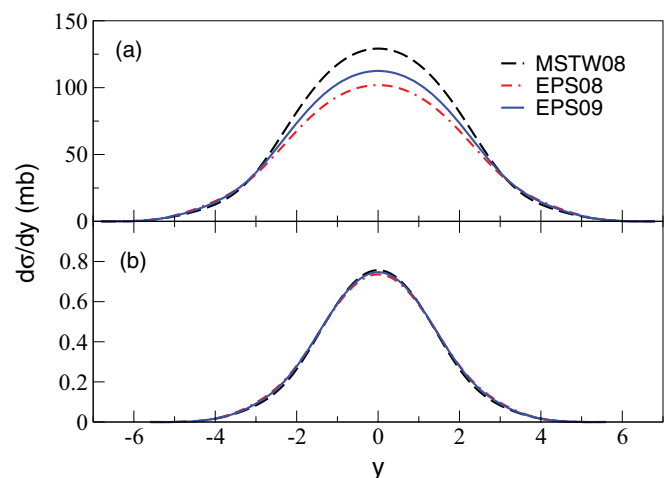


FIG. 2. (Color online) Rapidity distributions of the photoproduction of (a)  $c\bar{c}$  and (b)  $b\bar{b}$  in PbPb collisions at  $\sqrt{s_{NN}} = 2.76$  TeV using the GRV photon parton distributions. Dashed lines depict results using the MSTW08 parton distributions (no nuclear modifications). Solid and dash-dotted lines are results from nuclear-modified parton distributions from EPS09 and EPS08, respectively.

TABLE III. Cross sections for elastic photoproduction of  $J/\psi$  (in  $\mu\text{b}$ ) and  $\Upsilon$  (in nb) in ultraperipheral  $p\text{Pb}$  collisions.

|                               | PDF    | $\gamma p$ | $\gamma\text{Pb}$ | Total |
|-------------------------------|--------|------------|-------------------|-------|
| $J/\psi$<br>( $\mu\text{b}$ ) | MSTW08 | 63.6       | 18.3              | 81.9  |
|                               | EPS08  |            | 1.8               | 65.4  |
|                               | EPS09  |            | 6.6               | 70.2  |
|                               | HKN07  |            | 12.0              | 75.6  |
| $\Upsilon$<br>(nb)            | MSTW08 | 149.6      | 137.0             | 286.6 |
|                               | EPS08  |            | 54.8              | 204.4 |
|                               | EPS09  |            | 82.9              | 232.5 |
|                               | HKN07  |            | 101.5             | 251.1 |

discernible in the intervals  $3 < y < 5$  and  $-5 < y < -3$ , although the magnitude is rather small. As in  $p\text{Pb}$  collisions,  $b\bar{b}$  production shows little sensitivity to nuclear effects, with the resolved component being more significant.

We now present the results on the elastic photoproduction of  $J/\psi$  and  $\Upsilon(1s)$ . As discussed in Refs. [1,2] the production mechanism for these vector mesons involves the square of the nuclear/nucleon gluon distribution. This quadratic dependence leads to a dramatic increase in the sensitivity of both cross sections and rapidity distributions to nuclear effects (predominantly shadowing) on gluon distributions. In Table III we present the component and total cross sections for the elastic photoproduction of  $J/\psi$  and  $\Upsilon$  in ultraperipheral  $p\text{Pb}$  collisions at the LHC. The associated rapidity distributions are shown in Fig. 3.

Unlike the photoproduction of  $c\bar{c}$  and  $b\bar{b}$  in  $p\text{Pb}$  collisions, which is practically insensitive to shadowing, the enhanced sensitivity to gluon shadowing due to the quadratic dependence

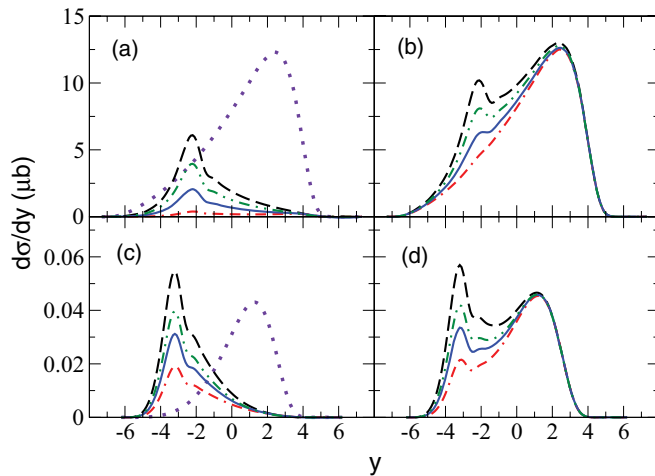


FIG. 3. (Color online) Rapidity distributions of the exclusive photoproduction of  $J/\psi$  [panels (a) and (b)] and  $\Upsilon$  [panels (c) and (d)] in  $p\text{Pb}$  collisions at  $\sqrt{s_{NN}} = 5$  TeV. Panels (a) and (c) show the  $\gamma p$  and  $\gamma\text{Pb}$  contributions separately while panels (b) and (d) show the sum. Dotted lines depict the  $\gamma p$  contributions while the dashed (MSTW08), dash-double-dotted (HKN07), solid (EPS09), and dash-dotted (EPS08) lines correspond to  $\gamma\text{Pb}$  contributions with no shadowing, weak shadowing, moderate shadowing, and strong shadowing respectively.

TABLE IV. Total cross sections for elastic photoproduction of  $J/\psi$  (in mb) and  $\Upsilon(1s)$  (in  $\mu\text{b}$ ) in ultraperipheral PbPb collisions.

| PDF    | $J/\psi$ (mb) | $\Upsilon$ ( $\mu\text{b}$ ) |
|--------|---------------|------------------------------|
| MSTW08 | 32.6          | 51.3                         |
| EPS08  | 6.3           | 32.2                         |
| EPS09  | 13.9          | 39.0                         |
| HKN07  | 22.1          | 41.3                         |

is already apparent here. Thus even though the  $\gamma p$  contribution is dominant in the case of  $J/\psi$  production, the  $\gamma\text{Pb}$  contributions from both MSTW08 (no shadowing) and HKN07 (weak shadowing) are still relatively appreciable. On the other hand the severity of the gluon shadowing present in EPS08 is enough to render its  $\gamma\text{Pb}$  contribution almost negligible. For  $\Upsilon(1s)$  production the  $\gamma\text{Pb}$  component contributes significantly and is in fact comparable to the  $\gamma p$  contribution in the case of MSTW08. Due to this, the effect of gluon shadowing is more clearly reflected in the total rapidity distributions and thus  $\Upsilon(1s)$  production may potentially be of some use in constraining gluon shadowing, especially in the  $-4 < y < -1$  rapidity interval.

The results on  $J/\psi$  and  $\Upsilon(1s)$  production in ultraperipheral PbPb collisions are presented in Table IV and Fig. 4. The differences in the predicted cross sections and rapidity distributions are markedly clear-cut, especially for  $J/\psi$ . Thus the photoproduction of  $J/\psi$  and  $\Upsilon(1s)$  in ultraperipheral PbPb collisions can serve as an excellent probe of gluon shadowing as well as a good discriminator of the different gluon shadowing sets utilized in the current study.

Let us briefly compare the present results to those at higher collision energies ( $p\text{Pb}$  at  $\sqrt{s_{NN}} = 8.8$  TeV and PbPb at  $\sqrt{s_{NN}} = 5.5$  TeV) presented in Ref. [2]. For  $p\text{Pb}$  collisions the cross sections for  $c\bar{c}$  ( $b\bar{b}$ ) production at  $\sqrt{s_{NN}} = 8.8$  TeV are approximately 1.8 (2.1) times those at  $\sqrt{s_{NN}} = 5.0$  TeV. The

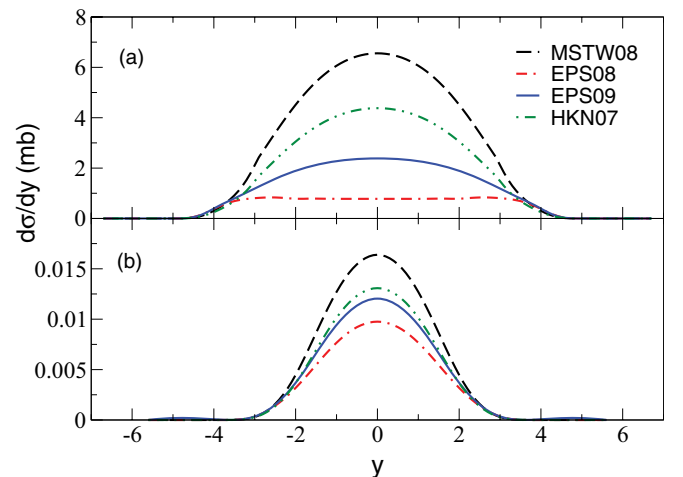


FIG. 4. (Color online) Rapidity distributions of the exclusive photoproduction of (a)  $J/\psi$  and (b)  $\Upsilon(1s)$  in PbPb collisions at  $\sqrt{s_{NN}} = 5.0$  TeV. Dashed, solid, dash-dotted, and dash-double-dotted lines are results from MSTW08, EPS09, EPS08, and HKN07 parton distributions, respectively.

relative  $\gamma$ Pb contributions are almost equal and nuclear effects are practically the same at both energies for both heavy quarks. For PbPb collisions the cross sections at  $\sqrt{s_{NN}} = 5.5$  TeV are approximately 2.1 (2.8) times those at  $\sqrt{s_{NN}} = 2.76$  TeV for  $c\bar{c}$  ( $b\bar{b}$ ). Nuclear effects are about 27% larger for  $c\bar{c}$  although shadowing trends are identical. The case of  $b\bar{b}$  is interesting: strong influence of antishadowing results in both EPS08 and EPS09  $b\bar{b}$  cross sections at  $\sqrt{s_{NN}} = 2.76$  TeV being larger than that of MSTW08. This contrasts with the behavior at  $\sqrt{s_{NN}} = 5.5$  TeV where the usual shadowing trend prevails.

Further differences manifest in the photoproduction of  $J/\psi$  and  $\Upsilon(1s)$  in  $p$ Pb collisions. For  $J/\psi$  the relative  $\gamma$ Pb contributions at  $\sqrt{s_{NN}} = 5.0$  TeV are about twice those at  $\sqrt{s_{NN}} = 8.8$  TeV and about 30% larger for  $\Upsilon(1s)$ . Shadowing effects are therefore more pronounced at lower energy and consequently better suited for constraining purposes. As expected total cross sections for  $J/\psi$  [ $\Upsilon(1s)$ ] are approximately a factor of 2.5 (2.2) larger than at  $\sqrt{s_{NN}} = 8.8$  TeV. For PbPb collisions although the cross sections are larger at  $\sqrt{s_{NN}} = 5.5$  TeV, the shadowing effects are almost the same (for  $J/\psi$ ) or slightly larger [for  $\Upsilon(1s)$ ] than at  $\sqrt{s_{NN}} = 2.76$  TeV. Thus the constraining abilities at both energies are almost at par.

In conclusion we offer the following remarks: the dependence on parton distributions is linear in the photoproduction

of heavy quarks and different modifications are superimposed due to the integration over the momentum fraction  $x$ . Despite these limitations, both cross sections and rapidity distributions for  $c\bar{c}$  in PbPb collisions manifest appreciable sensitivity to shadowing around midrapidity and very slight sensitivity to antishadowing at more forward and backward rapidities. Thus  $c\bar{c}$  photoproduction offers good constraining potential for shadowing. Both  $c\bar{c}$  and  $b\bar{b}$  total photoproduction cross sections and rapidity distributions in  $p$ Pb collisions show little sensitivity to nuclear modifications. The resolved components are however appreciable, especially for  $b\bar{b}$ , and are significantly dependent on the choice of photon parton distributions. Thus it seems feasible that they could be of some use in constraining photon parton distributions. The outlook for constraining gluon shadowing is better still in the case of vector meson production. Here the quadratic dependence on gluon modifications makes the elastic photoproduction of vector mesons particularly attractive for constraining purposes. In particular both the cross sections and rapidity distributions for  $J/\psi$  and  $\Upsilon(1s)$  photoproduction in PbPb collisions exhibit very good sensitivity to gluon shadowing.

We acknowledge support by the US Department of Energy (Grant No. DE-FG02-08ER41533) and the Research Corporation.

- 
- [1] A. Adeluyi and C. A. Bertulani, *Phys. Rev. C* **84**, 024916 (2011).
  - [2] A. Adeluyi and C. A. Bertulani, *Phys. Rev. C* **85**, 044904 (2012).
  - [3] C. A. Bertulani and G. Baur, *Phys. Rep.* **163**, 299 (1988).
  - [4] C. A. Bertulani, S. Klein, and J. Nystrand, *Annu. Rev. Nucl. Part. Sci.* **55**, 271 (2005).
  - [5] V. P. Goncalves and C. A. Bertulani, *Phys. Rev. C* **65**, 054905 (2002).
  - [6] B. Abelev *et al.* (ALICE Collaboration), *Phys. Rev. Lett.* **108**, 082001 (2012).
  - [7] G. Aad *et al.* (ATLAS Collaboration), *Nucl. Phys. B* **850**, 387 (2011).
  - [8] G. Aad *et al.* (ATLAS Collaboration), *Phys. Lett. B* **705**, 9 (2011).
  - [9] S. Chatrchyan *et al.* (CMS Collaboration), *Phys. Rev. Lett.* **107**, 052302 (2011).
  - [10] V. Khachatryan *et al.* (CMS Collaboration), *Eur. Phys. J. C* **71**, 1575 (2011).
  - [11] R. Aaij *et al.* (LHCb Collaboration), *Eur. Phys. J. C* **72**, 2025 (2012).
  - [12] R. Aaij *et al.* (LHCb Collaboration), *Eur. Phys. J. C* **71**, 1645 (2011).
  - [13] A. D. Martin, W. J. Stirling, R. S. Thorne, and G. Watt, *Eur. Phys. J. C* **63**, 189 (2009).
  - [14] K. J. Eskola, H. Paukkunen, and C. A. Salgado, *J. High Energy Phys.* **07** (2008) 102.
  - [15] K. J. Eskola, H. Paukkunen, and C. A. Salgado, *J. High Energy Phys.* **04** (2009) 065.
  - [16] M. Hirai, S. Kumano, and T. H. Nagai, *Phys. Rev. C* **76**, 065207 (2007).
  - [17] M. Gluck, E. Reya, and A. Vogt, *Phys. Rev. D* **46**, 1973 (1992).
  - [18] G. A. Schuler and T. Sjostrand, *Z. Phys. C* **68**, 607 (1995).
  - [19] F. Cornet, P. Jankowski, and M. Krawczyk, *Acta Phys. Polon. B* **35**, 2215 (2004).